

Kinematic Equations for Front Motion and Spiral-Wave Nucleation

Aric Hagberg^{a,1} Ehud Meron^{b,2}

^a*Center for Nonlinear Studies and T-7, Theoretical Division,
Los Alamos National Laboratory, Los Alamos, NM 87545*

^b*The Jacob Blaustein Institute for Desert Research and the Physics Department,
Ben-Gurion University, Sede Boker Campus 84990, Israel*

Abstract

We present a new set of kinematic equations for front motion in bistable media. The equations extend earlier kinematic approaches by coupling the front curvature with the order parameter associated with a parity breaking front bifurcation. In addition to naturally describing the core region of rotating spiral waves the equations can be used to study the nucleation of spiral-wave pairs along uniformly propagating fronts. The analysis of spiral-wave nucleation reduces to the simpler problem of droplet, or domain, nucleation in one space dimension.

1 Introduction

The onset of spatio-temporal disorder in reaction-diffusion systems is often accompanied by the spontaneous nucleation of spiral waves. The conditions for spiral-wave nucleation, mechanisms behind it, and implications on the resulting dynamics have been studied extensively [1–6]. Yet detailed studies of the nucleation process itself are still lacking. One difficulty in carrying out such studies stems from the two-dimensional structures of spiral waves. In this paper we report on the derivation of new kinematic equations for front motion in bistable media which reduce the two-dimensional spiral-wave nucleation problem to a one-dimensional droplet nucleation problem [7,8]. We use the kinematic equations to demonstrate the destabilization of traveling V-shape solutions to spiral nucleation.

The derivation is carried out in a parameter range that includes a pitchfork front bifurcation called a nonequilibrium Ising-Bloch (NIB) bifurcation [9–12]. At a NIB bifurcation, a stationary “Ising” front loses stability to a pair

¹ aric@lanl.gov

² ehud@bgumail.bgu.ac.il

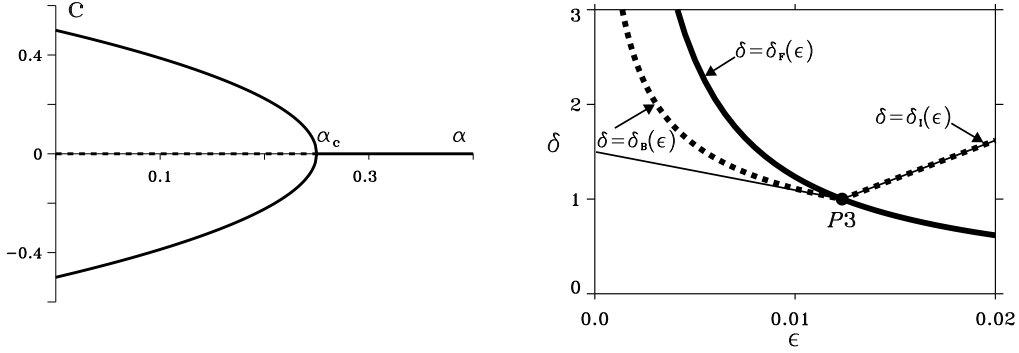


Fig. 1. (a) The nonequilibrium Ising-Bloch (NIB) front bifurcation. The solid line represents a branch of stable front solutions with speed c . At the bifurcation point, $\alpha = \alpha_c$, the stationary solution becomes unstable to a pair of counterpropagating fronts (b) The NIB front bifurcation and planar front transverse instability boundaries in the $\epsilon - \delta$ parameter plane. The thick line is the NIB bifurcation, $\delta_F(\epsilon)$, and the dashed lines are the boundaries for the transverse instability of Ising, $\delta_I(\epsilon)$, and Bloch, $\delta_B(\epsilon)$, fronts. Above these lines planar fronts are unstable to transverse perturbations. The thin lines are the approximations to the transverse instability boundaries obtained from the kinematic equations. Parameters: $a_1 = 4.0$, $a_0 = 0$.

of counter-propagating “Bloch” fronts as a parameter α is decreased past a critical value (Fig. 1a). The coexistence of the two Bloch fronts beyond the bifurcation allows for nucleation events where a front line segment of one Bloch type undergoes a transition to the other Bloch front.

The kinematic description of front motion consists of the following equations:

- An equation for the order parameter, C_0 , associated with the NIB bifurcation:

$$\frac{\partial C_0}{\partial t} = (\alpha_c - \alpha)C_0 - \beta C_0^3 + \gamma\kappa + \gamma_0 + \frac{\partial^2 C_0}{\partial s^2} - \frac{\partial C_0}{\partial s} \int_0^s \kappa C_n ds'. \quad (1)$$

- A geometric equation for the front curvature, κ :

$$\frac{\partial \kappa}{\partial t} = -(\kappa^2 + \frac{\partial^2}{\partial s^2})C_n - \frac{\partial \kappa}{\partial s} \int_0^s \kappa C_n ds'. \quad (2)$$

- An equation relating the normal front velocity C_n , the curvature κ , and the order parameter C_0 :

$$C_n = C_0 - D\kappa. \quad (3)$$

In these equations s is the front arc length and the critical parameter value α_c designates the NIB bifurcation point. The kinematic equations are derived for a FitzHugh-Nagumo model with a diffusing inhibitor. They generalize an

earlier kinematic approach [13,14] by treating C_0 as an independent dynamic mode rather than a constant.

The order parameter equation (1) yields the bifurcation diagram of Fig. 1a for planar (not curved) front solutions in a symmetric system ($\gamma_0 = 0$). The two Bloch branches pertain to high and low C_0 values, $C_0 = C_0^\pm \equiv \pm\sqrt{(\alpha_c - \alpha)/\beta}$. Because of the coupling between the order parameter and curvature equations, curvature variations are capable of nucleating low C_0 segments (droplets) in regions of high C_0 . Droplet nucleation in the kinematic equations corresponds to spiral-wave pair nucleation in the physical two-dimensional plane.

Spatially uniform front transitions induced by curvature, producing for example breathing spots, have been studied in Ref. [15,16]. The present paper is an extension of this earlier work to nonuniformly curved fronts. Complementary results to those reported here appear in Ref. [17].

2 Derivation of the kinematic equations

The curvature equation (2) follows from purely geometric considerations [13,14,18–20]. The normal velocity relation (3) and the order parameter equation (1) can be derived using the FitzHugh-Nagumo reaction-diffusion model with a diffusing inhibitor,

$$\begin{aligned}\frac{\partial u}{\partial t} &= \epsilon^{-1}(u - u^3 - v) + \delta^{-1}\nabla^2 u, \\ \frac{\partial v}{\partial t} &= u - a_1 v - a_0 + \nabla^2 v,\end{aligned}\tag{4}$$

where u and v , the activator and the inhibitor, are real scalar fields and ∇^2 is the Laplacian operator in two dimensions. The parameter a_1 is chosen so that (4) describes a medium with two stable spatially uniform states: an up state (u_+, v_+) and a down state (u_-, v_-) . Ising and Bloch front solutions connect the two uniform states (u_\pm, v_\pm) as the spatial coordinate normal to the front goes from $-\infty$ to $+\infty$. The remaining parameter space is spanned by ϵ, δ and a_0 , or alternatively by $\eta = \sqrt{\epsilon\delta}$, $\mu = \epsilon/\delta$, and a_0 . Note the parity symmetry $(u, v) \rightarrow (-u, -v)$ of (4) for $a_0 = 0$.

The NIB bifurcation line in the $\epsilon - \delta$ plane for $a_0 = 0$ is shown in Fig. 1b. For $\mu \ll 1$ it is given by $\delta = \delta_F(\epsilon) = \eta_c^2/\epsilon$, or $\eta = \eta_c$, where $\eta_c = \frac{3}{2\sqrt{2}q^3}$ and $q^2 = a_1 + 1/2$ [11]. The single stationary Ising front that exists for $\eta > \eta_c$ loses stability to a pair of counter-propagating Bloch fronts at $\eta = \eta_c$. Beyond the bifurcation ($\eta < \eta_c$) a Bloch front of an up state invading a down state coexists with another Bloch front of a down state invading an up state. Also shown in Fig. 1b are the transverse instability boundaries (for $a_0 = 0$), $\delta = \delta_I(\epsilon) = \epsilon/\eta_c^2$

and $\delta = \delta_B(\epsilon) = \eta_c/\sqrt{\epsilon}$, for Ising and Bloch fronts respectively. Above these lines, $\delta > \delta_{I,B}$, planar fronts are unstable to transverse perturbations [6,21]. All three lines meet at a codimension 3 point $P3$: $\epsilon = \eta_c^2$, $\delta = 1$, $a_0 = 0$.

The following assumptions are used in deriving Eqs. (3) and (1): $\mu = \epsilon/\delta \ll 1$, the front speed c is small, the front is weakly curved, and curvature variations along the front are weak. The second assumption is met by considering nearly symmetric ($|a_0| \ll 1$) systems and restricting parameter values to the Ising regime or the vicinity of the NIB bifurcation where the front speed is $c \propto \sqrt{\eta_c - \eta} \ll 1$. The last two assumptions are met by considering parameter values below or just beyond the threshold for the transverse instability of fronts.

The kinematic equations are derived by transforming to an orthogonal coordinate system that moves with the front and using singular perturbation theory with $\mu = \epsilon/\delta \ll 1$ as a small parameter [15]. The analysis of the narrow front core region, where u changes on a scale of order $\sqrt{\mu}$, gives equation (3) with

$$C_0 = -\frac{3}{\eta\sqrt{2}}v_f(s, t), \quad D = \delta^{-1}, \quad (5)$$

where $v_f(s, t)$ is the approximately constant value (in the direction normal to the front) of the inhibitor v in this region.

Away from the front core, where both u and v vary on a scale of order unity, a free boundary problem is obtained by using the solutions $u_{\pm}(v)$ of $u - u^3 - v = 0$ in the inhibitor (v) equation. Matching the solutions from each side of the front at the front core (in the limit $\mu \rightarrow 0$) gives the equation

$$\begin{aligned} \frac{\partial v_f}{\partial t} = & \frac{\sqrt{2}(\eta_c - \eta)}{q\eta_c^2}v_f - \frac{3}{4\eta_c^2}v_f^3 - \frac{4}{3}a_0 \\ & - \frac{2(1 - \delta^{-1})}{3q}\kappa + \frac{\partial^2 v_f}{\partial s^2} - \frac{\partial v_f}{\partial s} \int_0^s \kappa C_n ds'. \end{aligned} \quad (6)$$

Equation (6) coincides with (1) using the following identifications: $C_0 = -\frac{3}{\eta\sqrt{2}}v_f$, $\alpha = \frac{\eta\sqrt{2}}{q\eta_c^2}$, $\alpha_c = \frac{\sqrt{2}}{q\eta_c}$, $\beta = 1/6$, $\gamma = \alpha_c(1 - \delta^{-1})$, and $\gamma_0 = 2\alpha_c q a_0$. More details about the derivation appear in Ref. [17].

3 Numerical solutions of the kinematic equations

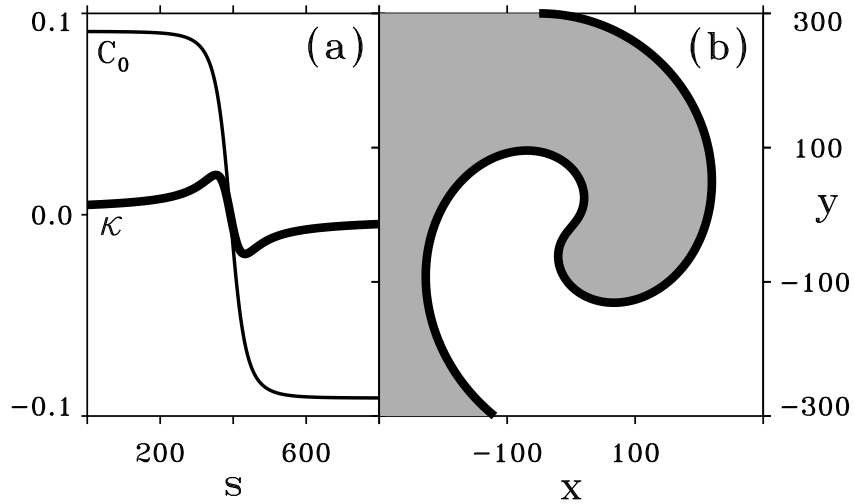


Fig. 2. A front solution to the kinematic equations (1)-(3). (a) The order parameter C_0 and the curvature κ along the arc length s . (b) In the $x-y$ plane the front solution corresponds to a rotating spiral wave. The shaded (light) region corresponds to an up (down) state. Parameters: $a_1 = 4.0$, $a_0 = 0$, $\epsilon = 0.01234$, $\delta = 1.0$.

3.1 Spiral waves

Consider a front solution in the kinematic equations that connects the state $C_0 = C_0^+$, $\kappa = 0$, at $s = -\infty$ with the state $C_0 = C_0^-$, $\kappa = 0$, at $s = +\infty$, where for a symmetric model ($a_0 = 0$ or $\gamma_0 = 0$) $C_0^\pm = \pm\sqrt{(\alpha_c - \alpha)/\beta}$. Fig. 2a shows such a solution obtained by numerically integrating (1)-(3). As demonstrated in Fig. 2b this front solution of the kinematic equations (1)-(3) represents a *spiral-wave* in the FitzHugh-Nagumo model (4). Unlike earlier kinematic approaches [13,14] the spiral core is naturally captured.

3.2 Traveling V-shape solutions and spiral-wave nucleation

For C_0 constant, the curvature equation (2) and the normal velocity relation (3) have a family of traveling V-shape solutions [20,22]

$$\kappa(s) = -\frac{b^2}{C_0 + C_n(0) \cosh(bs)}, \quad b^2 = C_n(0)^2 - C_0^2, \quad (7)$$

where $C_n(0) = C_0 - D\kappa(0)$ is an arbitrary constant. The traveling V-shape solution (7) is also an exact solution of the kinematic equations (1)-(3) for $\delta = 1$. In that case $\gamma = \alpha_c(1 - \delta^{-1}) = 0$ and the order parameter equation (1) decouples from the curvature equation for constant C_0 solutions. The specific values C_0 can assume are determined as solutions of the cubic equation $(\alpha_c - \alpha)C_0 - \beta C_0^3 + \gamma_0 = 0$.

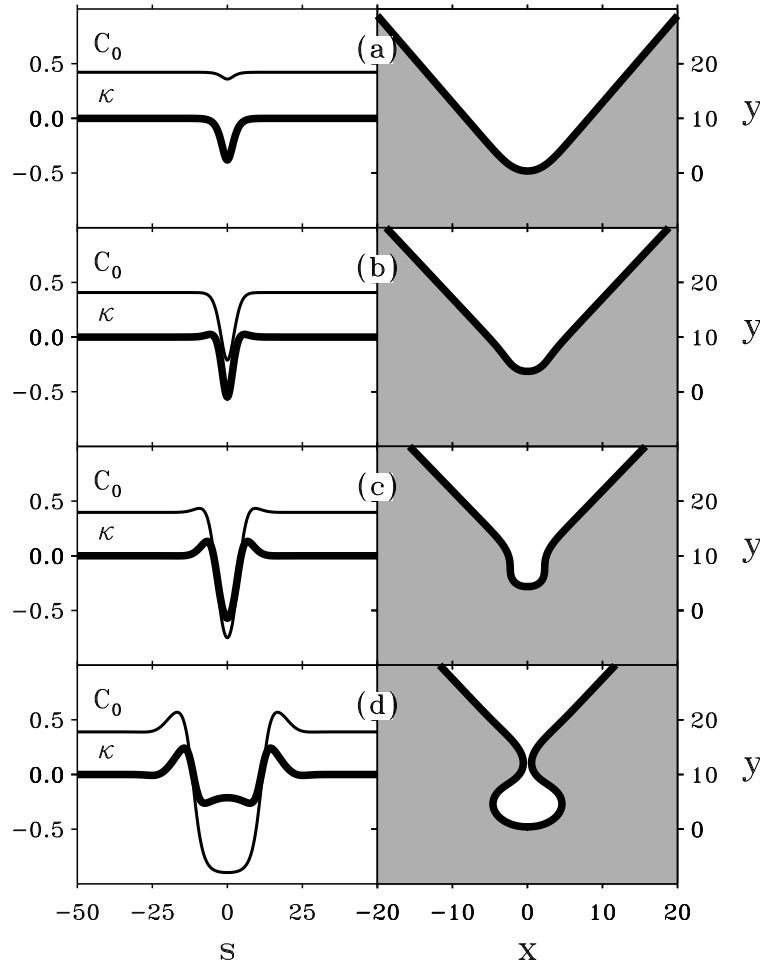


Fig. 3. Nucleation of a spiral-wave pair from an initial traveling V-shape front. Left column: the $C_0(s)$ and $\kappa(s)$ profiles. Right column: the front line shape in the $x - y$ plane. Parameters: $a_1 = 4.0$, $a_0 = -0.0001$, $\epsilon = 0.0115$, $\delta = 1.063$.

We have also found stable traveling V-shape numerical solutions for $\delta \neq 1$. Fig. 3a shows a V shape Bloch front traveling stably at constant speed. When approaching the NIB bifurcation (by increasing ϵ and/or δ) this solution becomes unstable and nucleates spiral-wave pair. The time evolution of an unstable V-shape solution is shown in Fig. 3(b-d).

We carried out numerical solutions of the FitzHugh-Nagumo model (4) to test the prediction, based on solutions of the kinematic equations, that traveling V-shape solutions are destabilized as the NIB bifurcation is approached. Choosing parameter values close to those of Fig. 3 an initial V form is indeed unstable and a pair of spiral-waves nucleate in the region of highest curvature as shown in Fig. 4. After the spirals form the resulting traveling fronts may either repel each other or reconnect and the V-shape solution will continue to propagate with the possible nucleation of new spiral pairs. Interactions between front segments are not included in the kinematic equations (1)-(3) so the resulting evolution of the spiral pair and possible front reconnections

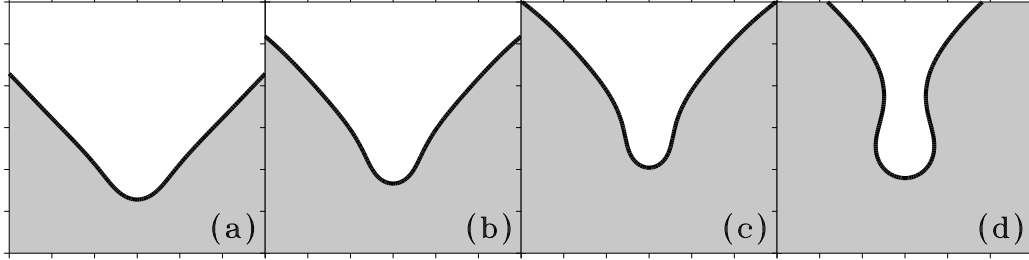


Fig. 4. Spiral-wave nucleation from an unstable traveling V-shape solution of the FitzHugh-Nagumo equations (4). The initial traveling V-shape solution (a) slows down (b) at the high curvature region and nucleates a pair of spiral waves (c). Depending on the parameters the resulting fronts may either repel or reconnect (d). Parameters: $\epsilon = 0.0122$, $\delta = 1.064$, $a_1 = 4.0$, $a_0 = -0.0001$.

cannot be captured. Front interactions have been studied recently in the fast inhibitor limit ($\eta \gg \eta_c$) [23].

4 Conclusion

The kinematic equations presented in this paper extend an earlier kinematic approach using the curvature equation (2) and a linear relation between the normal velocity and curvature [13,14]. Indeed, far into the Bloch regime (α significantly smaller than α_c), C_0 is no longer a slow degree of freedom and can be eliminated adiabatically. Equations (1) and (3) then reduce to a multivalued algebraic relation $C_0 = C_0(\kappa)$ whose three branches (two Bloch and one Ising) give approximately linear $C_n - \kappa$ relations [21].

But close to the NIB bifurcation C_0 becomes an active degree of freedom and the earlier approach, often called the “geometric approach”, is no longer valid. The new kinematic equations capture the core structures of spiral waves and spiral-wave nucleation processes. Since one space dimension has been eliminated in deriving the kinematic equations, the two-dimensional problem of spiral-wave nucleation has been reduced to a simpler droplet nucleation problem in one space dimension.

5 Acknowledgements

We wish to thank Paul Fife for many interesting discussions. This research was supported in part by grant No 95-00112 from the US-Israel Binational Science Foundation (BSF).

References

- [1] M. Courtemanche and A. T. Winfree, *Int. J. Bifurcation and Chaos* **1**, 431 (1991).
- [2] A. V. Holden and A. V. Panfilov, *Int. J. Bifurcation and Chaos* **1**, 219 (1991).
- [3] A. Karma, *Phys. Rev. Lett.* **71**, 1103 (1993).
- [4] M. Bär and M. Eiswirth, *Phys Rev. E* **48**, R1653 (1993).
- [5] M. Bär *et al.*, *Chaos* **4**, 499 (1994).
- [6] A. Hagberg and E. Meron, *Phys. Rev. Lett.* **72**, 2494 (1994).
- [7] J. D. Gunton and M. Droz, *Introduction to the Theory of Metastable States*, Vol. 183 of *Lecture Notes in Physics* (Springer-Verlag, Berlin, 1983).
- [8] P. C. Fife, *Mathematical Aspects of Reacting and Diffusing Systems*, Vol. 28 of *Lecture Notes in Biomathematics* (Springer-Verlag, New York, 1979).
- [9] P. Coullet, J. Lega, B. Houchmanzadeh, and J. Lajzerowicz, *Phys. Rev. Lett.* **65**, 1352 (1990).
- [10] H. Ikeda, M. Mimura, and Y. Nishiura, *Nonl. Anal. TMA* **13**, 507 (1989).
- [11] A. Hagberg and E. Meron, *Nonlinearity* **7**, 805 (1994).
- [12] M. Bode, A. Reuter, R. Schmeling, and H.-G. Purwins, *Phys Lett. A* **185**, 70 (1994).
- [13] A. S. Mikhailov, *Foundation of Synergetics I: Distributed Active Systems* (Springer-Verlag, Berlin, 1990).
- [14] E. Meron, *Physics Reports* **218**, 1 (1992).
- [15] A. Hagberg, E. Meron, I. Rubinstein, and B. Zaltzman, *Phys. Rev. E* **55**, 4450 (1997).
- [16] A. Hagberg and E. Meron, Technical report, Center for Nonlinear Studies, Los Alamos National Laboratory (unpublished).
- [17] A. Hagberg and E. Meron, *Phys. Rev. Lett.* **78**, 1166 (1997).
- [18] V. S. Zykov, *Simulation of Wave Processes in Excitable Media* (Manchester University Press, Manchester, 1987).
- [19] E. Meron and P. Pelcé, *Phys Rev. Lett.* **60**, 1880 (1988).
- [20] P. K. Brazhnik, *Physica D* **94**, 205 (1996).
- [21] A. Hagberg and E. Meron, *Chaos* **4**, 477 (1994).
- [22] P. K. Brazhnik and J. J. Tyson, *Phys. Rev. E* **54**, 4338 (1996).
- [23] R. E. Goldstein, D. J. Muraki, and D. M. Petrich, *Phys. Rev. E* **53**, 3933 (1996).